

High-pressure Catalytic Kinetics of CO₂ Reforming of Methane Over Highly Stable NiCo/SBA-15 Catalyst

Hao Wu,¹ Yajin Li,¹ Huimin Liu^{1,2,3*} and Dehua He^{1*}

Investigating the kinetic behaviors of catalysts in the reaction of CO₂ reforming of CH₄ (CRM) under industrially practical pressures is of great significance for designing stable catalysts for its industrialization. This study explores the kinetic behavior of 4.5Ni0.5Co/SBA-15-CD, a stable catalyst for pressurized CRM (2000 kPa), at a continuous flow-type fixed-bed quartz tube lining-Inconel tubular reactor under kinetically controlled conditions. The kinetic measurements suggested that the forward reaction rates were monotonically increasing with the partial pressures of CH₄ (200 – 400 kPa), and independent of the partial pressures of CO₂ (100 – 300 kPa) over 4.5Ni0.5Co/SBA-15 at 2000 kPa total pressure and 620–660 °C. The trace Co enriched on the outmost surface of NiCo particles of 4.5Ni0.5Co/SBA-15 facilitated the adsorption of co-reactant, and the decomposition of methane was the sole kinetically relevant step. Apparent activation energy of CRM reaction at high pressure measured on 4.5Ni0.5Co/SBA-15 was 106.5 kJ mol⁻¹ at total pressure of 2000 kPa.

Keywords: CO₂ reforming of methane; Ni-Co catalyst; High pressure; Kinetics

Received 22 November 2018, **Accepted** 25 January 2019

DOI: 10.30919/esee8c201

Funding:

Natural Science Foundation of China (21073104); National Basic Research Program, MOST China (2011CB201405); Australia Research Council discovery early career researcher award (DE180100523)

1. Introduction

The reaction of CO₂ reforming of methane (CRM) is important for the conversion of the two greenhouse gases, CO₂ and CH₄, into syngas (the mixture of CO and H₂), a valuable feedstock for the downstream production of clean fuels by the approach of Fischer-Tropsch Synthesis (FTS). Ni has been investigated as an active metal for the CRM reaction, but Ni-based catalysts also suffer from gradual deactivation during the CRM due to carbon deposition and metal sintering.^{1–3} Many researchers have been devoting a lot of effort trying to enhance the catalytic performance of Ni-based catalysts, including the support type and doping,^{4,8} modification of Ni metal,^{9–10} improvement of support and catalyst preparation methods,^{11–12} metal-support interaction^{13–14} and etc, and many remarkable results have also been achieved. On the other hand, from the industrial practical point of view, it is economic to perform pressurized CRM due to the following several reasons. (1) The exploitation, storage and transportation of natural gas (with the main component as methane), as well as the synthesis of chemicals via FTS are mostly carried out at high pressures. Then the pressure-bearing, CO-rich synthesis gas (H₂/CO < 1) obtained by the pressurized CRM reaction

could be used directly in industrial FTS processes.^{15–16} (2) The reactor used for pressurized CRM requires less volume and space and benefits for energy saving.^{17–18} (3) Pressurized H₂ (over 1000 kPa) is usually required by energy consumers, which makes it not economically desirable to compress large quantities of H₂ gas frequently.¹⁹ Therefore, studying pressurized CRM is one of the important research directions. Nevertheless, most of the reported researches were focused on CRM that carried out under atmospheric pressure,^{20–23} while the researches on high pressure CRM over Ni catalysts were relatively less reported. Aika *et al.*^{24–25} and Fujimoto *et al.*^{26–27} devoted a lot of effort to the studies on high pressure (1000 – 2000 MPa) CRM. Recently, we also reported a Co-modified Ni catalyst showed pretty good performance in pressurized CRM reaction.²⁸

Besides the researches on catalysts, investigating catalyst kinetic behaviours is a promising approach for providing insights for the development of stable catalyst. There have been multiple kinetic studies in atmospheric CRM, and different types of kinetic models were achieved. Maier *et al.* investigated the kinetics of CRM over Ir/Al₂O₃ in the range of 700–850 °C and a first order model was obtained by numerically fitting the experimental data with rate equations.²⁹ Nguyen *et al.* found that over Ni⁰/La₂O₃, the reaction order was constant in terms of CH₄ whereas was highly dependent on the concentration/pressure of CO₂.³⁰ While on the other hand, in spite of some contradictions on reactant activation and rate-determining step, Langmuir-Hinshelwood model have been suggested by several kinetic studies.³¹ For example, Bhatia *et al.* studied the reaction kinetics over Ni-Co bimetallic catalyst at different reactant partial pressures (0.045–0.36 MPa), and a kinetic model, the Langmuir-Hinshelwood model, was proposed that the adsorption and cracking of methane on metallic Ni particles was the rate-determining step, in which the reaction between CO₂ or its derived carbonate species with carbon existed at the interface of metal-carbon produced CO and removed the carbon deposited on the active metallic

¹Innovative Catalysis Program, Key Laboratory of Organic Optoelectronics and Molecular Engineering of Ministry of Education, Department of Chemistry, Tsinghua University, Beijing 100084, China

²School of Chemical and Biomolecular Engineering, The University of Sydney, NSW 2006, Australia

³TJU-NIMS International Collaboration Laboratory, School of Material Science and Engineering, Tianjin University, Tianjin 300072, China

*E-mail: hedeh@mail.tsinghua.edu.cn; huimin.liu@sydney.edu.au

catalyst surface.³¹ The Langmuir-Hinshelwood kinetic model was also proved on Rh/La₂O₃ by Cornaglia *et al.*³², on Co/Pr₂O₃ by Ayodele *et al.*³³ and on Ni/La/Al₂O₃ by Olsbye *et al.*³⁴. On the contrary, Osaki *et al.* suggested that over Ni based catalysts, such as Ni/MgO, Ni/Al₂O₃ and Ni/SiO₂, the rate-determining step in CRM was the reaction between CH_{x,ads} and CO (or O_{ads}).³⁵ Another type of Langmuir-Hinshelwood kinetics model was regarded as a better representative model for Co/La₂O₃ catalyst in CRM, in which both CH₄ and CO₂ were associatively adsorbed via a dual-site model followed by bimolecular surface reaction.³⁶

To the best of our knowledge, the kinetic behaviour of CRM over Ni-Co catalyst under industrial practical pressure conditions has not been reported in detail. Therefore, from the industrialization point of view, it will be of great significance to study the kinetic behaviour of CRM Ni-Co catalyst at pressurized conditions. Our group previous studies revealed that 4.5Ni0.5Co/SBA-15-CD catalyst prepared by the β -CD modified impregnation method has excellent activity and stability both in atmospheric and pressurized CRM reaction (2000 kPa, V(CH₄)/V(CO₂)=1:1, GHSV=3.0×10⁴ mL/g/h).^{10,28} Hence, in this paper, 4.5Ni0.5Co/SBA-15-CD is used as probe catalyst for studying pressurized CRM under kinetically controlled conditions. The effects of reaction conditions, especially reaction pressure, is explored and verified.

2. Experimental section

The reagents, such as Ni(NO₃)₂·6H₂O, Co(NO₃)₂·6H₂O, tetraethyl orthosilicate, β -cyclodextrin (β -CD), hydrochloric acid (HCl, 36~38 %), were used for preparing the catalyst, and the detailed manufacturer sources of the reagents could be referenced from our previous paper.²⁸ The standard gases with different CH₄/CO₂ ratios (Ar gas balance) were purchased from Beijing Hua Tong Jing Ke gas Co., Ltd.

The catalyst used for the pressurized CRM reaction, 4.5Ni0.5Co/SBA-15-CD, was prepared with the β -CD modified impregnation method,³⁷ and the preparation procedure can be seen in our previous work.²⁸ The total metal loading (Ni and Co) was theoretically kept as 5 %.

Table 1 Detail compositions of each standard gas.

Number	Composition (mol%)		
	CH ₄	CO ₂	Ar
1	50	50	0
2	10	10	80
3	5	10	85
4	15	10	75
5	20	10	70
6	10	5	85
7	10	15	75
8	10	20	70

The physico-chemical properties of 4.5Ni0.5Co/SBA-15-CD were characterized by N₂ adsorption-desorption isotherm, X-ray diffraction, Inductively coupled plasma-atomic emission spectroscopy, X-ray photoelectron spectroscopy, H₂-temperature programmed reduction methods and Transmission electronic microscopy, while the detailed characterization results have been shown in our previous paper.^{10,28}

The kinetic measurements of CRM reaction over 4.5Ni0.5Co/SBA-15-CD catalyst under the total pressure of 2000 kPa were conducted at a continuous flow-type fixed-bed quartz tube lining-Inconel tubular reactor, with schematic diagram of equipment available in our previous paper.²⁸ Before each reaction, gas leakage test was carried out with Ar gas at 2200 kPa to make sure no gas leaking. Before the CRM reaction, the catalyst was reduced in-situ in flowing 5 % H₂/Ar (20 mL/min) at atmospheric pressure and 700 °C for 1 h. The reactant gases were fed into the reactor at a given pressure. All eight types of CH₄ and CO₂ mixed gases (Ar gas balance) were served as feed gases in the kinetic measurements, and the detail compositions of each feed gas are listed in Table 1. The flow rate was monitored by mass flow controllers (MFC), and the reaction temperature was detected by inserting a thermocouple (TC) to the catalyst bed. All the operating procedures of pressurized CRM reaction, products analysis and the conversion and selectivity calculation methods are same as our previous work.²⁸

3. Results and discussion

3.1 Exclusion of internal and external transport artifacts for kinetic measurements

The stable performance of 4.5Ni0.5Co/SBA-15-CD catalyst under pressurized CRM (2000 kPa, V(CH₄)/V(CO₂)=1:1, GHSV=3.0×10⁴ mL/g/h) has been verified in our previous work.²⁸ Before the kinetic measurements, the methods of changing the flow rates of feed gas and the particle sizes of the catalyst are usually adopted to eliminate the external and internal transport artifacts. Therefore, the effects of flow rates of feed gas and the catalyst particle sizes on the reaction rate of 4.5Ni0.5Co/SBA-15-CD were checked, and the results are displayed in Fig. 1 and Fig. 2. It is clear that the external transport artifact could be eliminated by adopting the flow rate of feed gas more than 60 mL/min, and there is no influence of internal transport artifact if the particle size of catalyst is less than about 0.4 mm (>40 mesh). According to these results, 90 mL/min flow rate of feed gas and 40-60 mesh particle size of

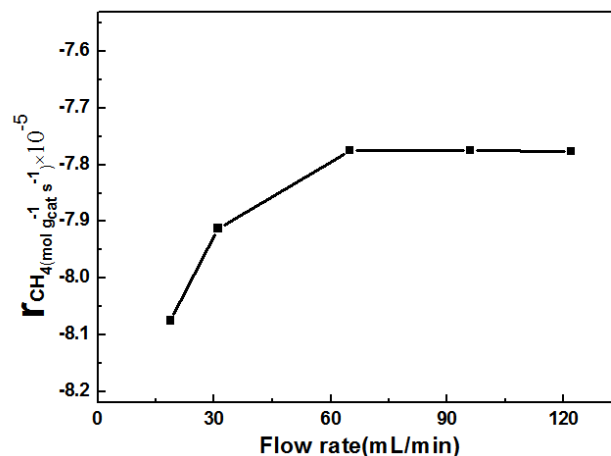


Fig. 1 Effect of flow rates on reaction rate of 4.5Ni0.5Co/SBA-15-CD. Reaction conditions: 660 °C, CO₂/CH₄/Ar=10/10/80, GHSV=3.6×10⁵ mL/g/h, catalyst diluted with 600 mg quartz, 2000 kPa total pressure.

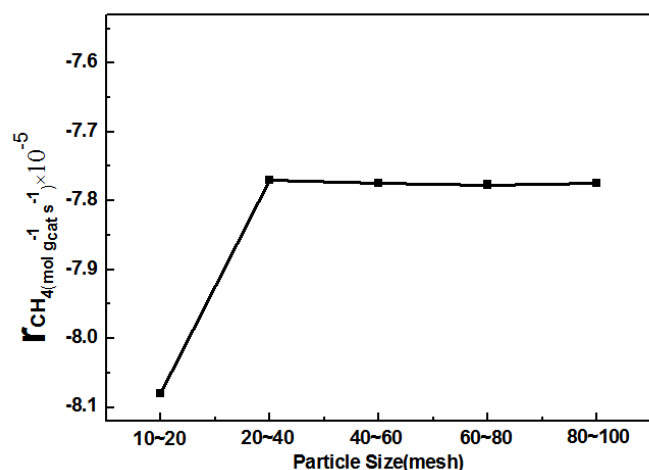


Fig. 2 Effect of particle sizes on reaction rate of 4.5Ni0.5Co/SBA-15-CD. Reaction conditions: 660 °C, CO₂/CH₄/Ar=10/10/80, GHSV=3.6×10⁵ mL/g/h, catalyst diluted with 600 mg quartz, 2000 kPa total pressure.

the catalyst were employed. So, the kinetic measurements of 4.5Ni0.5Co/SBA-15-CD catalyst were carried out at kinetically limited conditions: 15 mg catalyst diluted with 600 mg quartz, 40-60 mesh particle size, 90 mL/min total flow rate (total GHSV=3.6×10⁵ mL/g/h), 2000 kPa total pressure and 620-700 °C. The partial pressures of both CH₄ and CO₂ were kept in the range of 100 – 400 kPa.

3.2 Reaction kinetic studies over 4.5Ni0.5Co catalyst at a total pressure of 2000 kPa

In order to ensure the reliability of the kinetic measurements, the CH₄ reaction rates in pressurized CRM at the present study were kept at a low level (less than 20 % CH₄ conversion). The GHSV was as high as 3.6×10⁵ mL/g/h, so that the net rate measurements were far from the equilibrium. Based on the reaction conditions and the partial pressures of each substance under steady-state reaction, we could estimate the differences between the actual reaction states and the thermodynamic equilibrium states under the reaction conditions, which is called the reaction progress degree η , and it could be calculated according to the following equation.³⁸⁻³⁹

$$\eta = \frac{[P_{CO_2}]^2 [P_{H_2}]^2}{[P_{CH_4}] [P_{CO_2}]} \times \frac{1}{K_{EQ}}$$

where $[P_i]$ is the partial pressure for the reactant/product species i (in units of kPa) in CRM reaction, while $[K_{EQ}]$ is the equilibrium constant for CRM at the operating reaction temperature.

At the present study, η values were controlled in the range from 0.03 to 0.28, so the reactions were far from the equilibrium. The influence of CH₄ partial pressures on the pressurized CRM reaction rate was measured with fixing CO₂ partial pressure being 200 kPa while adjusting CH₄ partial pressure in the range of 200 ~ 400 kPa, under the condition of total pressure 2000 kPa (Ar as balance gas). Similarly, the influence of CO₂ partial pressures on the pressurized CRM reaction rate was measured with fixing CH₄ partial pressure being 200 kPa while adjusting CO₂ partial pressure in the range of 100 ~ 300 kPa, under the condition of total pressure 2000 kPa. The CRM reaction rate determined under the CRM experimental conditions with different temperatures and different partial pressures of the reactants was the net reaction rate r_n , while the forward reaction rate (r_f) could be obtained

from net reaction rate (r_n) and reverse reaction rate (r_r) using the following formula.³⁸⁻³⁹

$$r_n = r_f - r_r = r_f(1 - \eta)$$

Here, the net reaction rate was corrected for approach to reaction equilibrium (η), while η can be obtained from the equilibrium constant and prevalent pressures of reactants and products, and this equation described the observed effect of reactor residence time and CH₄ conversion level on the measured CRM rates, according to the research results by Iglesia *et al.*³⁸

Based on the obtained forward reaction rate (r_f), the effects of the partial pressures of CH₄ and CO₂ on the forward CH₄ conversion rate over 4.5Ni0.5Co/SBA-15-CD at 620-660 °C and 2000 kPa total pressure are shown in Fig.3 and Fig.4.

As it is clear from Fig. 3, the forward reaction rates of pressurized CRM were proportional to the partial pressure of CH₄ (200 – 400 kPa) at reaction temperatures of 620-660 °C over 4.5Ni0.5Co/SBA-15-CD

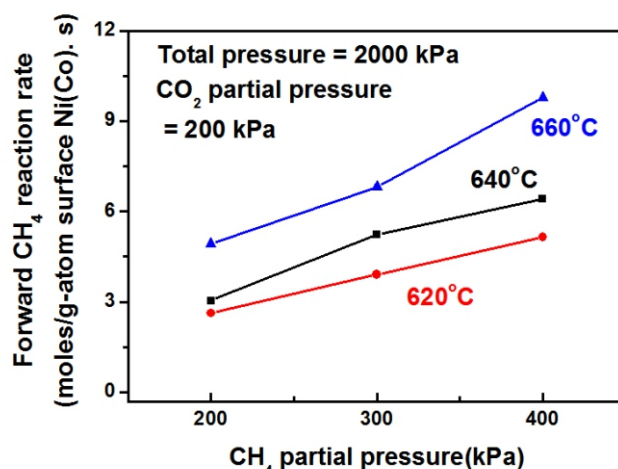


Fig. 3 Effects of CH₄ partial pressures on the forward CH₄ conversion rate in CRM over 4.5Ni0.5Co/SBA-15-CD. Reaction conditions: GHSV=3.6×10⁵ mL/g/h, balance gas Ar, 2000 kPa total pressure.

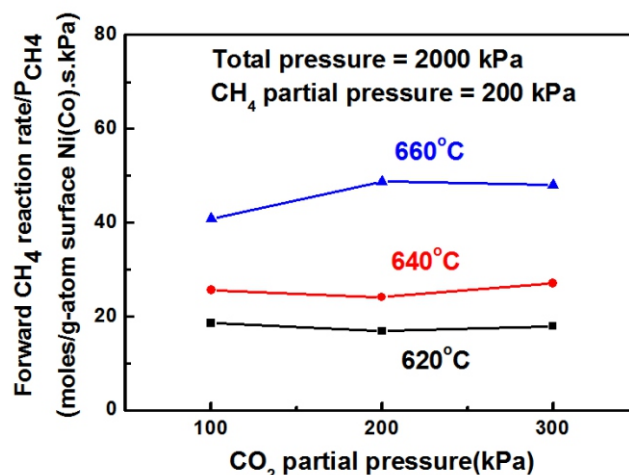


Fig. 4 Effects of CO₂ partial pressures on the forward CH₄ conversion rate in CRM over 4.5Ni0.5Co/SBA-15-CD. Reaction conditions: GHSV=3.6×10⁵ mL/g/h, balance gas Ar, 2000 kPa total pressure.

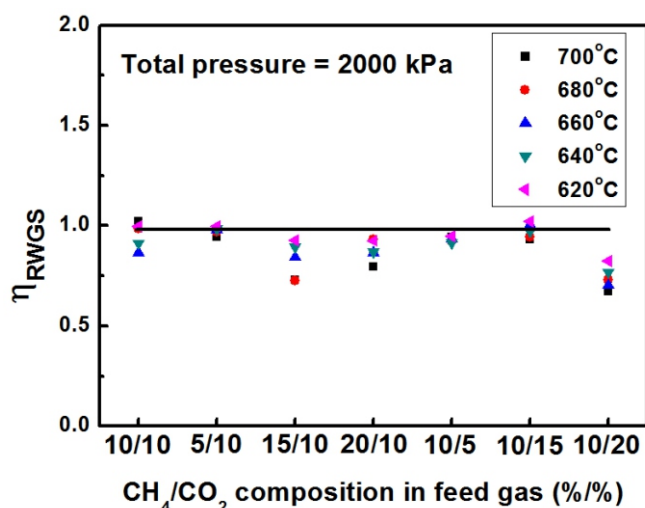


Fig. 5 Extent of RWGS equilibrium at varied reaction temperatures as a function of feed gas composition.

Reaction conditions: GHSV=3.6×10⁵mL/g/h, Ar gas balance, 2000 kPa total pressure.

under 2000 kPa total pressure. The proportional relationship was due to the reason that the frequency of CH₄ contacted with an active site per unit time was increased as the partial pressure of CH₄ increased, which increases the number of effective collisions of CH₄, thereby increasing the forward reaction rate. On the other hand, the forward reaction rate of pressurized CRM were independent of CO₂ partial pressures (100 – 300 kPa) at different temperatures (620 °C ~ 660 °C), as shown in Fig. 4. The independence reaction rate on CO₂ partial pressure might be due to the reason that the elementary steps of CO₂ adsorption and the surface reaction between the adsorbed species CO₂* and CH₄ decomposed species CH_{4,x}* were fast steps, which approached the reaction equilibrium, so that the partial pressures of CO₂ did not affect the forward reaction rate. These results mentioned above are agreed with the reported kinetics for supported metal catalysts mentioned in the literature, and it was also confirmed that the co-reactant CO₂ and the partial pressures of the products CO and H₂ had no influence on the forward reaction rate in the CRM reaction.³⁸⁻⁴³

The side reaction, reverse water-gas shift reaction (RWGS, CO₂+H₂=CO+H₂O) would occur unavoidably during CRM reaction. The extent of RWGS equilibrium (η_{RWGS}) at different temperatures as a function of the composition of feed gas was calculated with the following equation,³⁸⁻³⁹ $\eta_{RWGS} = ([P_{CO}][P_{H_2O}]) / ([P_{CO_2}][P_{H_2}]K_{RWGS})$, where $[K_{RWGS}]$ is the equilibrium constant of RWGS reaction at the operating reaction temperature, by assuming the $[P_{H_2O}]$ equals to the equilibrium calculated, as shown in Fig. 5. The value of η_{RWGS} closes to unity suggesting that all the RWGS relevant elementary steps were fast steps. These results clearly indicated that CH₄ activation was the only kinetically controlled elementary step over 4.5Ni0.5Co/SBA-15-CD catalyst even under high pressures (~2000 kPa). The desorption of hydrogen and CO, as well as the reaction of CH_{4,x}* species with CO₂* were fast steps, so that the RWGS would be equilibrated under the present reaction conditions.³⁸

Based on the fact that the forward CH₄ reaction rate was proportional to the partial pressure of CH₄ while independent of the partial pressure of CO₂ and CH₄ activation was the only kinetically controlled elementary step, the CRM reaction rates over 4.5Ni0.5Co/SBA-15-CD under the pressure of 2000 kPa could be expressed as

$$r_f = kP_{CH_4}$$

This rate equation is first-order to CH₄ and zeroth-order to CO₂, which is in good consistency with the results reported by Iglesia *et al.*, and the partial pressures of H₂ and CO have no effect on r_f .³⁸⁻³⁹

3.3 Apparent activation energy over 4.5Ni0.5Co catalyst at high pressure

The apparent activation energy of CRM reaction was measured over 4.5Ni0.5Co/SBA-15-CD at high pressure (2000 kPa), and the results are illustrated in Fig. 6. The measured activation energy of 106.5 kJ/mol was close to the reported values for 7%Ni/MgO (105kJ/mol)³⁹ and Ni/SiO₂ (96.3 kJ/mol),⁴⁴ suggesting that the rate-determining step occurred mainly on Ni surface in 4.5Ni0.5Co/SBA-15-CD. Therefore, we speculated that the CO in 4.5Ni0.5Co/SBA-15-CD catalyst facilitated the adsorption of CO₂ and was mainly covered with the adsorbed CO₂* or O* species, while the trace Co in the catalyst enhanced the catalyst stability by preventing sintering.⁴⁵

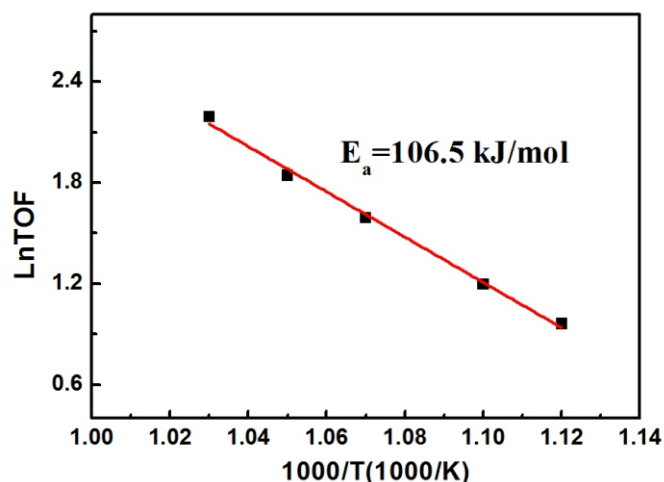


Fig. 6 Arrhenius plots under high pressures in CRM over 4.5Ni0.5Co/SBA-15-CD. The apparent activation energy is shown in the insets.

3.3 Comparison between the kinetic studies over 4.5Ni0.5Co/SBA-15-CD catalyst under high pressure CRM with literatures

Some examples of the kinetic equations of CRM in previous studies from literatures are summarized in Table 2. Apparently, the kinetic equations obtained under atmospheric CRM might vary with the catalytic reaction systems. In the case that the reaction follows a Langmuir-Hinshelwood kinetic model, the equation used to express reaction rate might be relatively complicated (No. 1 in Table 2 is an example). In comparison, $r_{CH_4} = k(P_{CH_4})^y(P_{CO_2})^z(P_{H_2O})^w$ or $r_{CH_4} = k(P_{CH_4})^y(P_{CO_2})^z$ might be a more general form for the kinetic equations,⁴⁶⁻⁴⁷ with y and z values of zero or nearly zero being achieved over Ir/ZrO₂, Ni/Kieselguhr, La_{2-x}Sr_xNiO₄ perovskite-type oxides. Then the equation could be simplified as $r_{CH_4} = k(P_{CH_4})^y$, which is quite similar to the one obtained in our study of 4.5Ni0.5Co/SBA-15-CD in pressurized CRM, suggesting that CH₄ cracking was the sole kinetically controlled step in this study.

4. Conclusions

In this study, the catalytically stable 4.5Ni0.5Co/SBA-15-CD was used as a probe catalyst for kinetic study in pressurized CRM. The forward

Table 2 Kinetic equations in previous studies under atmospheric CRM.

No	Equation	Description	Ref.
1	$-r_{CH_4} = \frac{K_1 K_2 K_3 K_4 P_{CH_4} P_{CO_2}}{K_1 K_3 K_4 P_{CH_4} P_{CO_2} + K_1 K_2 P_{CH_4} + K_3 K_4 P_{CO_2}}$	Over Ni-X bimetallic catalysts, where X=Ca, K, Ba, La and Ce.	[31]
	<p>K_1 is the methane adsorption equilibrium constant, K_2 is the methane decomposition (cracking) rate constant on the metallic surface, K_3 is the adsorption equilibrium constant of CO_2 on the binary support to form the surface carbonate, K_4 is the reaction rate constant between the carbon deposited on the surface of metallic clusters and the surface carbonate species.</p>		
2	$r_{CH_4} = kP_{CH_4}$	Over Rh/ Al_2O_3 , Ni/MgO, Pt/ ZrO_2 , Ir/ ZrO_2 , Ru/ Al_2O_3 catalysts	[38-43]
3	$r_{CH_4} = k(P_{rCH_4})^\alpha (P_{CO_2})^\beta (P_{H_2O})^\gamma$	Over Ni/La/ Al_2O_3 catalyst. Among the reaction orders for CH_4 , CO_2 , H_2O , and H_2 , only the reaction order for CH_4 was not zero, and the reaction orders could be affected by the promoters.	[46]
4	$r_{CH_4} = k (P_{CH_4})^{m1} (P_{CO_2})^{n1}$	Over $La_{2-x}Sr_xNiO_4$ catalyst. $m1 = 0.41 - 0.89$, $n1$ nearly zero.	[47]
5	$r_{CH_4} = kP_{CH_4}$	Over 4.5Ni0.5Co/SBA-15, under a total of 2000 kPa	Present work

reaction rates were found to be proportional with the CH_4 partial pressures (200 – 400 kPa) and unrelated to CO_2 partial pressures (100 – 300 kPa) on 4.5Ni0.5Co/SBA-15-CD at 620-660 °C and 2000 kPa total pressure, confirming that the activation of methane was the kinetically relevant step. This study will provide some reference for designing industrially practical catalysts for pressurized CRM.

Acknowledgements

We acknowledge financial support for this work from Natural Science Foundation of China (21073104) and the National Basic Research Program, Ministry of Science and Technology of China (973 Program, 2011CB201405). Huimin Liu acknowledges the financial support from Australia Research Council discovery early career researcher award (DE180100523). Hao Wu acknowledges the support of the Australian and Western Australian Governments and the North West Shelf Joint Venture Partners, as well as the Western Australian Energy Research Alliance (WA:ERA).

Reference

- D. Chen, R. Lodeng, A. Anundskas, O. Olsvik and A. Holmen, *Chem. Eng. Sci.*, 2001, **56**, 1371-1379.
- B. Pawelec, S. Damyanova, K. Arishtirova, J. L. G. Fierro and L. Petrov, *Appl. Catal. A*, 2007, **323**, 188-201.
- Z. Li, L. Mo, Y. Kathiraser and S. Kawi, *ACS Catal.*, 2014, **4**, 1526-1536.
- H. M. Liu, Y. M. Li, W. W. Yang, H. Wu and D. H. He, *Chin. J. Catal.*, 2014, **35**, 1520-1528.
- M. Ocsachoque, J. Bengoa and D. Gazzoli, *Catal. Lett.*, 2011, **141**, 1643-1650.
- C. E. Daza, C. R. Cabrera and S. Moreno, *Appl. Catal. A*, 2010, **378**, 125-133.
- J. Q. Zhu, X. X. Peng and L. Yao, *Int. J. Hydro. Energ.*, 2011, **36**, 7094-7104.
- M. Ikeguchi, T. Mimura, Y. Sekine, E. Kikuchi and M. Matsukata, *Appl. Catal. A*, 2005, **290**, 212-220.
- J. Huang, R. Ma, Z. Gao, C. Shen and W. Huang, *Chin. J. Catal.*, 2012, **33**, 637-644.
- H. Wu, H. M. Liu, W. W. Yang and D. H. He, *Catal. Sci. Technol.*, 2016, **6**, 5631-5646.
- Y. Li, Q. Ye, J. M. Wei and B. Q. Xu, *Chin. J. Catal.*, 2004, **25**, 326-330.
- H. M. Liu, Y. M. Li, H. Wu, J. X. Liu and D. H. He, *Chin. J. Catal.*, 2015, **36**, 283-289.
- M. C. J. Bradford and M. A. Vannice, *Catal. Today*, 1999, **50**, 87-96.
- M. A. Goula, A. A. Lemonidou and A. M. Efstathiou, *J. Catal.*, 1996, **161**, 626-640.
- M. E. Dry, *Catal. Today*, 2002, **71**, 227-241.
- H. Jahangiri, J. Bennett, P. Mahjoubi, K. Wilson and S. Gu, *Catal. Sci. Technol.*, 2014, **4**, 2210-2229.
- Y. F. Zhang, G. J. Zhang and B. M. Zhang, *et al. Chem. Eng. J.*, 2011, **173**, 592-597.
- J. B. Zhao, Y. D. Li and L. Tian, *et al. Chin. J. Catal.*, 1998, **19**, 491-493.
- J. N. Armor and D. J. Martenak, *Appl. Catal. A*, 2001, **206**, 231-236.
- H. Zhou, T. Zhang, Z. Sui, Y. Zhu, C. Han, K. Zhu and X. Zhou, *Appl. Catal. B: Environ.*, 2018, **233**, 143-159.
- W. Yin and S. S. C. Chuang, *Catal. Commun.*, 2017, **102**, 62-66.

22. B. AlSabban, L. Falivene, S. M. Kozlov, A. Aguilar-Tapia, S. Ould-Chikh, J. L. Hazemann, L. Cavallo, J. M. Basset and K. Takanabe, *Appl. Catal. B: Environ.*, 2017, **213**, 177-189.
23. Z. H. Bao, Y. W. Lu and F. Yu, *AIChE Journal*, 2017, **63**, 2019-2029.
24. K. Nagaoka, K. Takanabe and K. Aika, *Chem. Commun.*, 2002, **9**, 1006-1007.
25. K. Nagaoka, K. Takanabe and K. Aika, *Appl. Catal. A*, 2003, **255**, 13-21.
26. K. Tomishige, Y. Himeno, Y. Matsuo, Y. Yoshinaga and K. Fujimoto, *Ind. Eng. Chem. Res.*, 2000, **39**, 1891-1897.
27. K. Tomishige, Y. Himeno, O. Yamazaki, Y. Chen, T. Wakatsuki and K. Fujimoto, *Kinet. Catal.*, 1999, **40**, 388-394.
28. H. Wu, J. X. Liu, H. M. Liu and D. H. He, *Fuel*, 2019, **235**, 868-877
29. M. F. Mark, F. Mark and W. F. Maier, *Chem. Eng. Technol.*, 1997, **20**, 361-370
30. T. H. Nguyen, L. Agata and K. Andrzej, *Appl. Catal. B*, 2015, **165**, 389-398.
31. M. S. Fan, A. Z. Abdullah and S. Bhatia, *ChemSusChem*, 2011, **4**, 1643-1653.
32. J. F. Munera, S. Irusta and L. M. Cornaglia, *J. Catal.*, 2007, **245**, 25-34.
33. B. V. Ayodele, S. B. Abdullah and C. K. Cheng, *Int. J. Hydro. Energ.*, 2017, **42**, 28408-28424
34. U. Olsbye, T. Wurzel and L. Mleczko, *Ind. Eng. Chem. Res.*, 1997, **36**, 5180-5188.
35. T. Osaki, T. Horiuchi and K. Suzuki, *J. Chem. Soc. Fara. T.*, 1996, **92**, 1627-1631.
36. B. V. Ayodele, M. R. Khan, S. S. Lam and C. K. Cheng, *Int. J. Hydro. Energ.*, 2016, **41**, 4603-4615.
37. H.M. Liu, Y.M. Li, H. Wu, H. Takayama, T. Miyake and D. H. He, *Catal. Commun.*, 2012, **28**, 168-173.
38. J. M. Wei and E. Iglesia, *J. Catal.*, 2004, **225**, 116-127.
39. J. M. Wei and E. Iglesia, *J. Catal.*, 2004, **224**, 370-383.
40. J. M. Wei and E. Iglesia, *Angew Chem. Int. Edit.*, 2004, **43**, 3685-3688.
41. J. M. Wei and E. Iglesia, *J. Phys. Chem. B*, 2004, **108**, 4094-4103.
42. J. M. Wei and E. Iglesia, *J. Phys. Chem. B*, 2004, **108**, 7253-7262.
43. J. M. Wei and E. Iglesia, *Phys. Chem. Chem. Phys.*, 2004, **6**, 3754-3759.
44. M. C. J. Bradford and M. A. Vannice, *Appl. Catal. A*, 1996, **142**, 97-122.
45. E. Nikolla, J. Schwank and S. Linic, *J. Catal.*, 2007, **250**, 85-93
46. M. H. Park, B. K. Choi and Y. H. Park, *J. Nanosci. Nanotechnol.*, 2015, **15**, 5255-5258.
47. C. Pichas, P. Pomonis and D. Petrakis, *Appl. Catal. A*, 2010, **386**, 116-123.